VOL. 22, NO. 2, 2023, 30-36
elektrika.utm.my
ISSN 0128-4428

ELEKTRIKA
Journal of Electrical Engineering

A Compact Metamaterial Dual-band Branch-line Coupler for 5G Applications

Abdulkadir Bello Shallah[1*], **Farid Zubir**[1*], **Mohamad Kamal A. Rahim**[2], **Mohamad Rijal Hamid**[2], **Arshad Karimbu Vallappi**[3], **Huda A. Majid**[4], **Zubaida Yusoff**[5] and **Abdul Basit**[6,7]

[1]Wireless Communication Centre, Faculty of Electrical Engineering, Universiti Teknologi Malaysia, 81310 Johor Bahru, Johor, Malaysia.
[2]Advanced RF & Microwave Research Group (ARFMRG), Faculty of Electrical Engineering, Universiti Teknologi Malaysia, 81310 Johor Bahru, Johor, Malaysia.
[3]Department of Electrical Engineering, Faculty of Engineering, Islamic University of Madinah, Saudi Arabia.
[4]Faculty of Engineering Technology, Pagoh Higher Education Hub, Universiti Tun Hussein Onn Malaysia, 84600 Pagoh, Johor, Malaysia.
[5]Faculty of Engineering, Multimedia University, Persiaran Multimedia, 63100 Cyberjaya, Selangor, Malaysia.
[6]School of Information Science and Engineering, NingboTech University, Ningbo 315100, China.
[7]College of Information Science and Electronic Engineering, Zhejiang University, Hangzhou 310027, China.

[*]Corresponding author: shallah@graduate.utm.my and faridzubir@utm.my

Abstract: This study introduces a compact branch-line coupler (BLC) based on metamaterial (MTM) technology that can operate in sub-6 GHz 5G frequency bands. Conventional vertical and horizontal sections of the BLC were replaced with T-shaped TLs and interdigital capacitor (IDC) unit cells incorporated into the BLC sections to improve their performance and reduce their dimensions. The BLC is designed on a Rogers RT5880 substrate material, and it operates at dual frequencies of 0.7 GHz and 3.5 GHz. The design was simulated using CST Microwave Studio software and achieved enhanced frequency band ratio.

Keywords: Branch-line coupler, Dual-band, Frequency ratio, interdigital capacitor, metamaterial

Article History: received 18 April 2023; accepted 13 August 2023; published 28 August 2023.

1. INTRODUCTION

The use of millimeter-wave and microwave telecommunications is becoming increasingly popular for processing large volumes of data in 5G and next-generation communication systems [1]. Couplers are commonly used in applications involving RF, microwave, and millimeter-wave frequencies, with branch-line couplers (BLCs) being particularly prominent among the various types of couplers available [2]. Couplers play a crucial role in several applications, such as Doherty power amplifiers [3], balanced power amplifiers [4], and balanced mixers [5]. Additionally, they can be employed for power splitting in numerous other applications [6].

To miniaturize couplers, traditional methods involve substituting transmission lines (TLs) with their lumped-element equivalents [7] or using high-permittivity substrates [8]. Another compelling option is to use step impedance [9] and additional stubs instead of the conventional TLs [10]. Meanwhile, a crucial element in creating a multiband system that is necessary for advancing and improving the wireless communication sector is the multiband BLC. Various techniques and structures have been utilized to develop dual-band BLC. These include T-shaped TLs, as described in [11, 12], PI-shaped [13], center-tapped stubs [14], and coupled lines [15]. All of the aforementioned techniques exhibit dual-band operation capability; however, each has its limitations. Some feature large structure sizes or small frequency ratios, whereas others possess narrow bandwidths and undesirable high insertion losses.

The emergence of metamaterial (MTM) structures has paved the way for a new range of applications in microwave and millimeter-wave circuits [16]. Composite right/left-handed (CRLH) TLs possess highly desirable features, such as enhanced component miniaturization, dual-band functionality, increased bandwidth, and zeroth-order resonance. Thus, a significant number of researchers have employed MTM unit cells to reduce the size, enable dual-band functionality, and enhance the electrical characteristics of BLCs [17-22].

This paper proposes a compact dual-band BLC with improved frequency band ratio, that operates in the lower 5G frequency bands of 0.7 GHz and 3.5 GHz. Conventional BLC shunts and series branches have been substituted with T-shaped TLs, which feature folded arms and stubs to achieve size reduction. In addition, an MTM structure using IDC unit cells was incorporated into the BLC section to enhance its performance and decrease its

overall size. The proposed structure was designed and simulated using the CST-MW studio.

2. PROPOSED DESIGN PROCEDURE

Figure 1 illustrates a conventional BLC consisting of two horizontal and vertical sections, with lengths equal to $\lambda/4$, and characteristic impedances of Z_o and $Z_o/\sqrt{2}$ respectively. Traditional TL are replaced with T-shaped TLs with a configuration comprising two TL sections (Z_a, θ_a), along with an open stub of (Z_b, θ_b). To achieve the dual-band function and reduce the overall circuit size, the electrical lengths of the TL sections and open stubs were made equal. The relationship between the $\lambda/4$ −TL and T-shaped lines can be expressed by equating their ABCD matrices, as described in [23, 24].

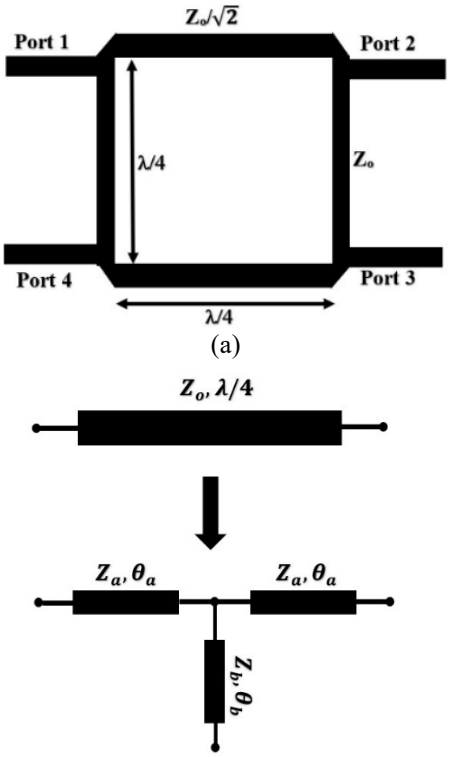

Figure 1. The diagram of (a) Conventional BLC (b) Modified T-shaped TLs.

2.1 Horizontal BLC section $(50/\sqrt{2}\ \Omega)$

Figure 2(a) illustrates the configuration of the horizontal T-shaped dual-band TL, and its frequency and phase responses are shown in Figures 2(b) and 2(c), respectively. From the figure 2(b), it can be seen that the horizontal TL allows the signal to pass through at 0.7 GHz and 3.5 GHz without, or negligible attenuation (S_{21} close to zero) and the S_{11} parameter is less than -10dB at both 0.7 GHz and 3.5 GHz frequency bands respectively. Likewise, Figure 2(c) shows that the $-90°$ and $+90°$ phases are realized at the desired frequencies of 0.7 GHz and 3.5 GHz, respectively. The total dimensions of the traditional horizontal TL are $(52.1\ mm \times 53.5\ mm)$ which is quite large and need to be miniaturized while maintaining its performance.

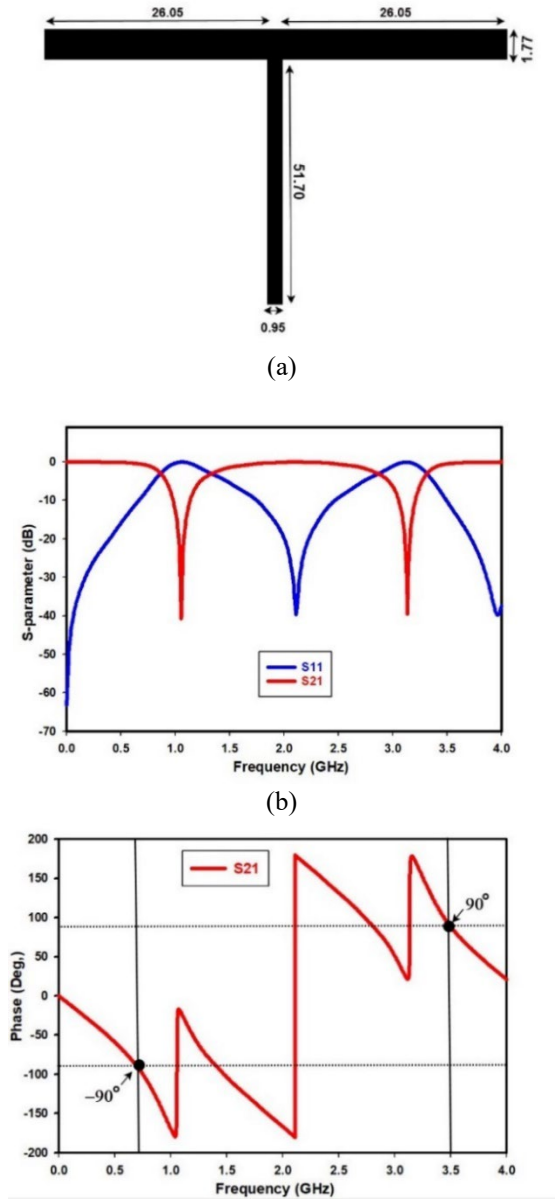

Figure 2. The conventional dual-band horizontal branch (a) Layout of the TL (b) S-parameters magnitude. (c) Phase response

2.2 Vertical BLC section $(50\ \Omega)$

The structure of the vertical T-shaped dual-band TL is illustrated in Figure 3(a). The total size of the vertical TL is obtained as $(54.4\ mm \times 55.3\ mm)$. The S-parameter and phase response of the vertical line are shown in Figure 3(b) and (c), respectively. Figure 3(b) illustrates that the signal can pass through the vertical line with minimal or no attenuation (S_{21} close to zero) at both 0.7 GHz and 3.5 GHz frequencies, and the S_{11} value is below -10dB for both frequency bands. Similarly, Figure 3(c) indicates that the $-90°$ and $+90°$ are achieved at the intended frequencies of 0.7 GHz and 3.5 GHz, respectively.

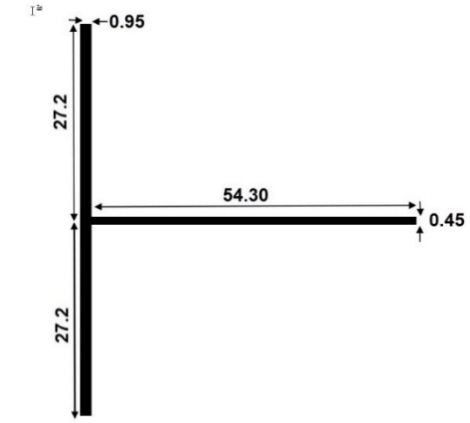

(a)

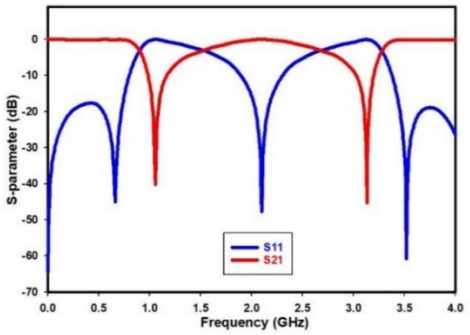

(b)

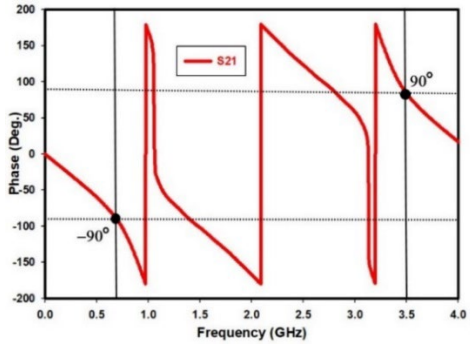

(c)

Figure 3. The conventional dual-band vertical branch (a) Layout of the TL (b) S-parameters magnitude. (c) Phase response

2.3 Proposed metamaterial-based BLC design

2.3.1 Interdigital capacitor (IDC)

Figure 4(a)–(c) show the unit cell of the IDC metamaterial structure and its equivalent circuits at both high and low frequencies. The IDC fingers have an overall base width of *Bw* and base length of *Bl*. The spacing between fingers is *s,* and *g* represents the gap at the end of the finger. In addition, the finger width and length are denoted by *fw* and *fl*, respectively.

The rough approximation for the total capacitance of the IDC is given by Equation (1) [25]:

$$C = (\varepsilon_r + 1) fl\,[(N-3)A_1 + A_2]\,(pF) \quad (1)$$

In Equation (1), *N* denotes the number of fingers, and the relative permittivity of the substrate material is represented as ε_r. The interior and exterior fingers of the IDC are represented by the constants A_1 and A_2 respectively, in relation to *h* and *Bw.* These values can be obtained using Equations (2) and (3):

$$A_1 = 4.409 \tanh\left[0.55\left(\frac{h}{Bw}\right)^{0.45}\right] \times 10^{-6}\ (pF/\mu m) \quad (2)$$

$$A_1 = 9.92 \tanh\left[0.52\left(\frac{h}{Bw}\right)^{0.5}\right] \times 10^{-6}\ (pF/\mu m) \quad (3)$$

where *Bw* and *h* represent the base width of the IDC fingers and the height of the substrate, respectively. Similarly, the parasitic resistance *R* resulting from conductor loss can be determined using Equation (4).

$$R = \frac{4}{3}\frac{fl}{fwN} R_s\ (\Omega) \quad (4)$$

Equations (5) and (6) determine the capacitance (C_s) and inductance (L) based on the assumption that *fw/h* << 1, where *c* is the velocity of light in vacuum [18].

$$L = \frac{Z_o\sqrt{\varepsilon_{eff}}}{c} fl\ \text{(H)} \quad (5)$$

$$C_s = \frac{1}{2}\frac{\sqrt{\varepsilon_{eff}}}{Z_o c} fl\ \text{(F)} \quad (6)$$

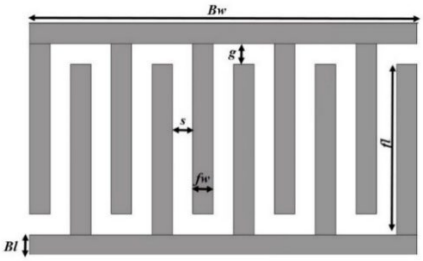

(a)

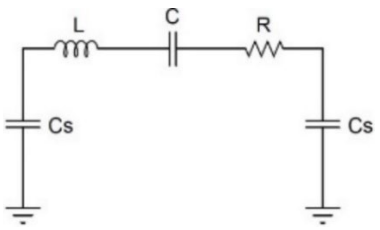

(b)

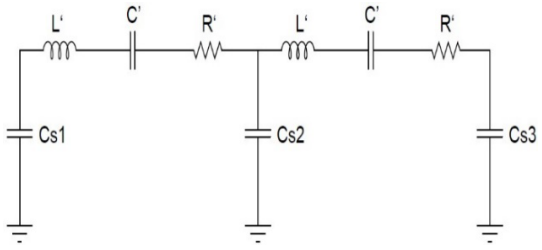

(c)

Figure 4. The layout diagram showing (a) geometry of the IDC. (b) low-frequency circuit equivalent (c) high-frequency circuit equivalent.

The geometrically optimized dimensions of the IDC are listed in Table 1.

Table 1. Interdigital capacitor dimensions

Parameter	*Bw*	*Bl*	*fl*	*fw*	*g*	*s*
Horizontal line IDC (35.3Ω)	5.7	0.3	2.5	0.3	0.3	0.3
Vertical line IDC (50 Ω)	5.7	0.3	2.5	0.3	0.3	0.3

2.3.2 Meandered microstrip line

The process of reducing the size of the BLC involves making several modifications to the stubs and branches, which are originally quite long. These modifications consist of incorporating an IDC unit cell, as shown in Figure 4(a), and adding multiple 90° bends to both stubs and branches, as depicted in Figure 5.

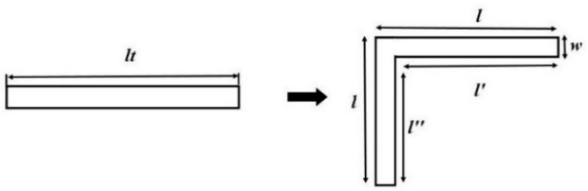

Figure 5. Application of a 90° bend in a straight TL

Equations (7) and (8) determine the process by which the bends are added to straight TLs.

$$l'' = l - w \tag{7}$$

$$lt = l' + l'' = w \tag{8}$$

where *w* and *lt* are the width and total length of a straight line, respectively. Truncating the edges helps reduce the impact of the extra capacitance generated by the discontinuity in the TL caused by the bends [26].

2.3.3 Proposed miniaturized MTM horizontal TL

Figure 6(a) shows the design layout of the proposed horizontal TL, which has IDCs on both sides and includes four 90° bends to increase compactness. The overall dimensions of the proposed horizontal TL are ($35.2\ mm \times 14.2\ mm$), which is 82.1% size reduction compared to the standard horizontal TL. The S-parameter and frequency responses to the proposed horizontal TL are shown in Figures 6(b) and 6(c), respectively. The results indicate that the proposed TL can effectively transmit signals at both 0.7 GHz and 3.5 GHz, similar to the horizontal TL in section 2. Additionally, it demonstrates that the desired phases $-90°$ and $+90°$ are achieved at frequencies of 0.7 GHz and 3.5 GHz, respectively.

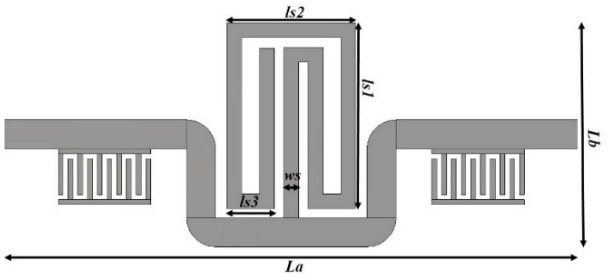

(a)

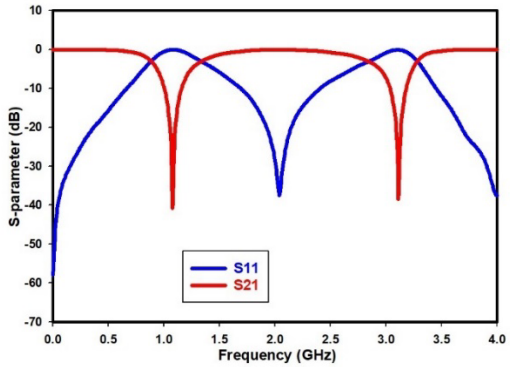

(b)

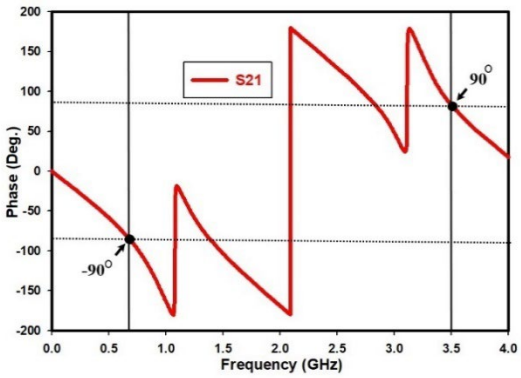

(c)

Figure 6. The proposed dual-band horizontal line (a) physical layout (b) S-parameter response (c) phase response

2.3.4 Proposed miniaturized MTM vertical TL

Figure 7(a) shows the design layout of the proposed vertical TL. This miniaturized TL includes IDCs on both sides and features four 90° bends to increase compactness. The proposed vertical TL covered a total dimension of ($35.8\ mm \times 12.7\ mm$). That is approximately 84.9% size reduction compared with the conventional vertical TL. The S-parameter and frequency responses are shown in Figures 7(b) and 7(c), respectively. According to the results, the proposed TL is capable of transmitting signals at both 0.7 GHz and 3.5 GHz, which is similar to the vertical TL in Section 2. Furthermore, it demonstrates that the intended phases of $-90°$ and $+90°$ are achieved at frequencies of 0.7 GHz and 3.5 GHz, respectively.

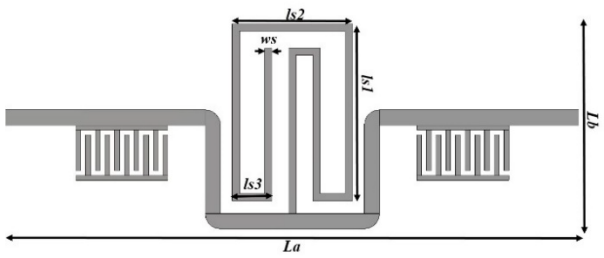

(a)

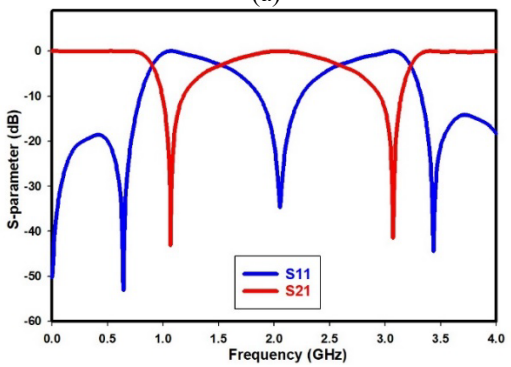

(b)

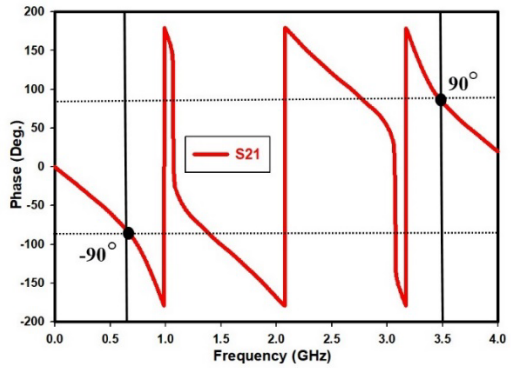

(c)

Figure 6. The proposed dual-band vertical line (a) physical layout (b) S-parameter response (c) phase response

Table 2 lists the physical dimensions of the proposed miniaturized TL sections, which are used to replace the vertical and horizontal TL sections of the conventional BLC.

Table 2. Proposed miniaturized TL dimensions

Parameter	***La***	***Lb***	***ls1***	***ls2***	***ls3***	***ws***
Horizontal line (35.3Ω)	35.2	14.2	11.7	7.9	2.9	0.9
Vertical line (50 Ω)	35.8	12.7	11.0	7.5	2.6	0.45

Using the CST-microwave studio as a full-wave simulator, the miniaturized MTM TL was designed with an IDC and meandered stub structure for both 35.3 Ω and 50 Ω lines. At 0.7 GHz and 3.5 GHz, the phases of −90° and +90° are achieved for both TLs. This can be used to replace conventional branches of the BLC to effectively reduce the size and enhance the performance of the proposed BLC.

2.3.5 miniaturized dual-band BLC

The proposed BLC operates in dual-band frequencies of 0.7 GHz and 3.5 GHz, and its design involves modifying the size of the TLs and open stubs to obtain the desired performance while also miniaturizing the overall structure size. Figure 8 illustrates the proposed device, which is 80% smaller than that of the traditional dual-band BLC in the same frequency bands.

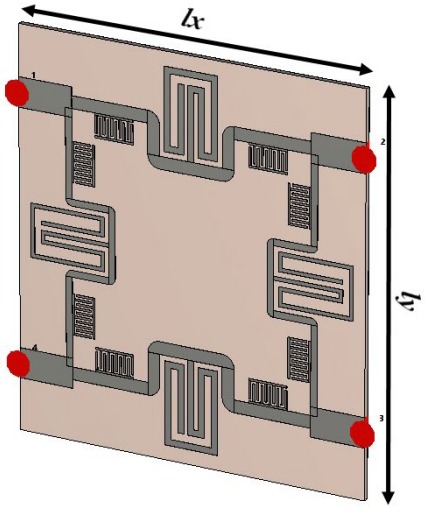

Figure 8. The layout diagram of the proposed dual-band BLC. (lx = 51.7 mm, ly = 55.05 mm)

3. SIMULATION RESULTS AND DISCUSSION

The S-parameters and phase response of the proposed BLC with respect to the output and isolated ports are shown in Figures 9 (a)–(c), respectively. The simulated results of the S-parameters in Figures 9 (a) and (b) indicate that the BLC can operate at the sub-6 GHz, 5G dual frequency bands of 0.7 GHz and 3.5 GHz. The proposed BLC exhibits return loss (S_{11}) and isolation loss (S_{41}) below -10 dB for both frequency bands. To achieve equal power distribution at the output coupled and through ports, the insertion loss (S_{21}) and coupling loss (S_{31}) should be approximately -3 dB. The simulated (S_{21}) and (S_{31}) of the proposed design as presented in Figure 9 (b) are -3.2 dB and -3.01 dB at 0.7 GHz, and -3.17 dB and 2.96 dB at 3.5 GHz frequency bands, respectively.

Similarly, optimal power distribution requires a phase difference of 90° between output ports 2 and 3. The simulated phase differences ($\angle S_{31}$ - $\angle S_{21}$) shown in Figure 9 (c) are 88.9° and 91.2° at 0.7 GHz and 3.5 GHz frequency bands, respectively. This implies that there was a maximum phase deviation of 1.2° between the two frequency bands.

Table 3 presents a performance comparison between the proposed BLC and other state-of-the-art designs in the literature.

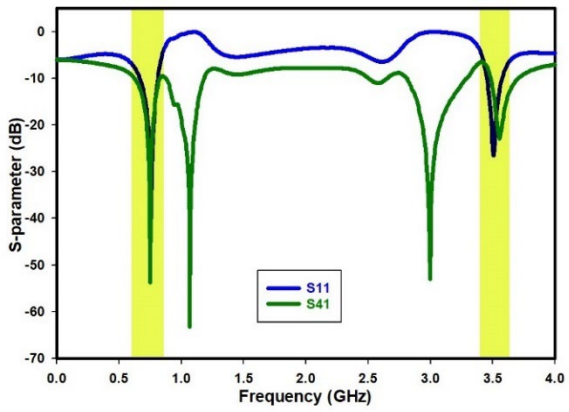

(a)

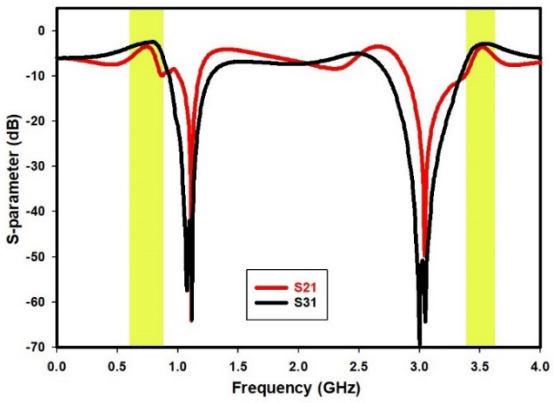

(b)

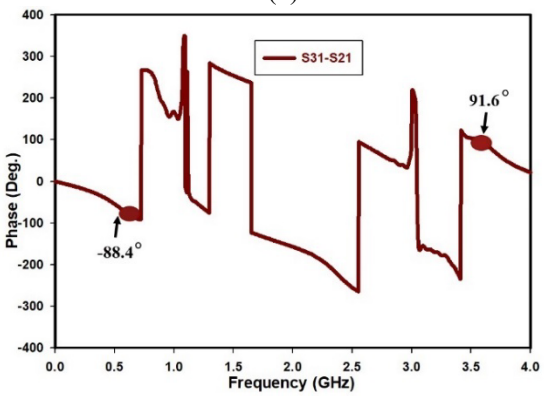

(c)

Figure 9. The S-parameter frequency response (a) the S_{11} and S_{41} (b) the S_{21} and S_{31} (c) Phase difference ($\angle S_{31}$ - $\angle S_{21}$)

Table 3. Proposed miniaturized TL dimensions

Ref.	*f (GHz)*	*S_{11} (dB)*	*S_{21} (dB)*	*S_{31} (dB)*	*Freq. ratio*	*Size (mm)*
[20]	2/3	-	-	-	1.5	57 mm × 63 mm
[21]	2.4/5.2	40.17/42.12	-3.79/-3.81	-2.74/-3.55	2.16	0.29 λ_g × 0.3 λ_g
[22]	2.4/5.2	30.5/16.1	--	-	2.16	20 mm × 21 mm
This work	0.7/3.5	25.2/20.1	-3.2/-3.17	-3.01/-2.96	5	51 mm × 55 mm

3. CONCLUSION

In this study, an MTM-based dual-band BLC with an enhanced frequency ratio was introduced. To achieve dual-band functionality, the TL sections of the traditional BLC were transformed into T-shaped TLs at the arms using ABCD matrix analysis. The design structure is further reduced in size by incorporating IDC unit cells into the BLC sections and meandering both arms and stubs, resulting in an approximately 80% reduction in the overall dimensions, while also improving its performance. In addition, this compact structure can be used in sub-6 GHz, 5G applications.

ACKNOWLEDGMENT

This research was funded by Higher Institution Centre of Excellence (HICOE), Ministry of Higher Education Malaysia through Wireless Communication Centre (WCC) Vot. No. R.J090301.7823.4J610. This work was also partially supported by the Universiti Teknologi Malaysia (UTM) under UTM Encouragement Research Grant (20J65) and UTMShine Batch 5 Grants (09G97)

REFERENCES

[1] Salh, A, Audah L, Abdullah O, Alhartomi M.A, Alsamhi S.H, Almalki F.A, Shah N.S.M. "Low computational complexity for optimizing energy efficiency in mm-wave Hybrid Precoding System for 5G" in *IEEE Access*, vol. 10, 2021, pp. 4714–4727.

[2] Lalbakhsh, A. Chen, Mohamadpour, G. et. al. "Design of a compact planar transmission line for miniaturized Rat-Race coupler with harmonics suppression." *IEEE Access*, vol. 9, 2021, pp. 129207–129217.

[3] Zhang Z, Cheng Z, Liu G, "A power amplifier with large high-efficiency range for 5G communication" *Sensors*, vol. 2020, 20. 5581,

[4] Powell, J.R.; Shepphard, D.J.; Quaglia, R.; Cripps, S.C. "A Power Reconfigurable High-Efficiency X-Band Power Amplifier MMIC Using the Load Modulated Balanced Amplifier Technique" *IEEE Microw. Wirel. Compon. Lett*, vol.28, 2018, pp. 527–529.

[5] Mohyuddin, W.; Kim, I.B.; Choi, H.C.; Kim, K.W. "Design of A Compact Single-Balanced Mixer for UWB Applications," *J. Electromagn. Eng. Sci*. vol. 17, 2007, pp. 65–70.

[6] Jamshidi, M.B. Roshani, S. et. al, "Size reduction and performance improvement of a microstrip Wilkinson power divider using a hybrid design technique" *Sci. Rep*. 2021, 11, 7773.

[7] Kurgan, P.; Filipcewicz, J.; Kitlinski, M. "Development of a compact microstrip resonant cell aimed at efficient microwave component size reduction" *IET Microw. Ant. Prop.* vol. 6, 2012, pp. 1291–1298.

[8] Hou, J.-A.; Weng, Y.-H. "Design of compact 90 and 180 couplers with harmonic suppression using lumped-element bandstop resonators" *IEEE Trans. Microw. Theory Tech*. vol. 58. 2010, pp. 2932–2939.

[9] Lalbakhsh, A.; Alizadeh, S.M. et al. "A Design of a Dual Band Bandpass Filter Based on Modal Analysis

for Modern Communication Systems. Electronics, 2020. 19, 1770.

[10] Liao, S.-S.; Sun, P.-T. et. al. "A novel compact-size branch-line coupler." *IEEE Microw. Wirel. Comp. Lett.* 2005, vol. 15, 588–590.

[11] H. Zhang and K. J. Chen, ''A stub tapped branch-line coupler for dual-band operations,'' *IEEE Microw. Wireless Compon. Lett.,* vol. 17, no. 2, pp. 106–108, Feb. 2007.

[12] H. Ren, J. Shao, M. Zhou, B. Arigong, J. Ding, and H. Zhang, ''Design of dual-band transmission line with flexible phase shifts and its applications,'' *IET Electron. Lett.,* vol. 51, no. 3, pp. 261–262, Feb. 2015.

[13] K.-K. M. Cheng and F.-L. Wong, ''A novel approach to the design and implementation of dual-band compact planar 90◦ branch-line coupler,'' *IEEE Trans. Microw. Theory Techn.*, vol. 52, no. 11, pp. 2458–2463, Nov. 2004.

[14] M.-J. Park, ''Dual-band, unequal length branch-line coupler with center-tapped stubs,'' *IEEE Microw. Wireless Compon. Lett*., vol. 19, no. 10, pp. 617–619, Oct. 2009.

[15] A. M. Zaidi, B. K. Kanaujia, M. T. Beg, J. Kishor, K. Rambabu, ''A novel dual-band branch line coupler for dual-band Butler matrix,'' *IEEE Trans. Circuits System, II, Exp. Briefs*, Dec. 2018.

[16] C. Caloz and T. Itoh, "Electromagnetic Metamaterials: Transmission Line Theory and Microwave Applications," New York: Wiley-IEEE Press, 2006.

[17] R. M. Khattab and A. A. T. Shalaby, "Metamaterial-Based Broadband Branch-line Coupler and its Application in a Balanced Amplifier," *2021 international Conference on Electronic Engineering (ICEEM),* Menouf, Egypt, 2021, pp 1-7.

[18] AK Vallappil, MKA Rahim, "Metamaterial based Compact Branch-line Coupler with Enhanced Bandwidth for use in 5G Applications," *The Applied Computational Electromagnetics Society Journal (ACES),* 2020, 35(6), 700-708.

[19] D. K. Choudhary, "Design of CRLT-TL Based Compact Hybrid Coupler Loaded with S-shaped Slot," *2021 6th International Conference for Convergence in Technology (12CT),* Maharashtra, India. 2021, pp. 1-4.

[20] R. Keshavarz, M. Danaeian, "A Compact Dual-Band 3 dB Branch Line Coupler Based on Interdigital Transmission lines," *2011 19th Iranian Conference on Electrical Engineering,* IEEE, (2011) pp. 1-5.

[21] P. Bhowmik, T. Moyra, "A Low-Cost Compact Planar Dual-Band 3 dB Branch Line Coupler Using an Unbalanced CRLH," *Iranian Journal of Science and technology, Trans. Of Elect, Engrn.* (2019) 43: 397-404.

[22] Khattak, M.K., Lee, C., Park, H., and Kahng, S. (2020). "A fully-printed CRLH dual-band dipole antenna fed by a compact CRLH dual-band balun," *Sensors*, *2020*(17), p.4991.

[23] A. B. Shallah, F. Zubir, M. K. A. Rahim, A. Abubakar, Z. Yusoff and M. Aminu-Baba, "A Miniaturized Branch Line Coupler for 5G Dual Band Applications," *2022 International Symposium on Antennas and propagation (ISAP),* Sydney, Australia, 2022, pp. 513-514.

[24] A. S. Mohra, "Dual Band Branch Line Coupler Using T and PI sections," no. June, 2016.

[25] C. Caloz and T. Itoh, Unk Electromagnetic Metamatrials: Transmission Line Theory and Microwave Applications, *Wiley and IEEE Press,* Hoboken, NJ, 2005.

[26] S. Singh, R. P. Yadav, A. Jain, "Miniaturized Dual-Band Branch-line Coupler with Folded Stubs." 5th *International Conference for Convergence in Technology (12CT)*, Pune, India. 2019.